ESAIM: M2AN 51 (2017) 1783–1803
DOI: 10.1051/m2an/2017009

ESAIM: Mathematical Modelling and Numerical Analysis
www.esaim-m2an.org

A PENALTY METHOD FOR A LINEAR KOITER SHELL MODEL

Ismail Merabet[1] and Serge Nicaise[2]

Abstract. In this paper a penalized method and its approximation by finite element method are proposed to solve Koiter's equations for a thin linearly elastic shell. In addition to existence and uniqueness results of solutions of the continuous and the discrete problems we derive some *a priori* error estimates. We are especially interested in the behavior of the solution when the penalty parameter goes to zero. We propose here a new formulation that leads to a quasi optimal and uniform error estimate with respect to the penalized parameter. In other words, we are able to show that this method converges uniformly with respect to the penalized parameter and to the mesh size. Numerical tests that validate and illustrate our approach are given.

Mathematics Subject Classification. 74K25, 65N30, 74S05.

Received April 22, 2016. Accepted March 7, 2017.

1. Introduction

Linear models of thin elastic shells can be classified into two different families: the Kirchhoff−Love theory and the Reissner−Mindlin theory. The Reissner−Mindlin plates theory was generalized to shells by P. M. Naghdi [24]. In the framework of the Kirchhoff−Love theory, Koiter [19] derived a two dimensional model for linearly elastic shells. The comparison between Koiter's and Naghdi's model leads to the comparison between the Kirchhoff−Love and Reissner−Mindlin theories. For "moderately" thin shells, the Naghdi model is better than the Koiter model, because it takes in account the transverse shear. Naghdi's model is also preferred because it better represents boundary conditions (it can distinguish between hard and soft simple support). But for very thin shells and for very smooth solutions, Koiter's model is better than Naghdi's model. Koiter's model is actually one of the most currently used for numerical computations, it contains both membrane and bending effects coupled at different order of magnitudes. W.T Koiter based his derivation on two *a priori* assumptions, one of a mechanical nature about the stresses inside the shell during the deformation. It states that if the thickness is small enough, then the state of stress is approximately planar and parallel to the tangent plane to the middle surface S. The second *a priori* assumption is of geometrical nature and states that the normal vector to the undeformed middle surface, considered as a set of particles of the shell, remains on a line normal to the deformed middle surface and the lengths are unmodified along this line after the deformation has taken place. For very thin elastic shells, Koiter's model was rigorously justified (see [15, 16]). For the classical formulation,

Keywords and phrases. Shell theory, Koiter's model, finite elements error analysis.

[1] LMA, Université Kasi Merbah – Ouargla, 30000, Algérie. merabet.ismail@univ-ouargla.dz

[2] LAMAV, Université de Valenciennes et du Hainaut-Cambrésis, Valenciennes cedex 9, France. serge.nicaise@univ-valenciennes.fr

Article published by EDP Sciences

the problem was formulated by the use of the covariant and contravariant components representation of the unknowns and a huge literature is dedicated to its approximation by various finite element methods. This formulation requires that the shell has a C^3-middle surface at least, which is restrictive from the point of view of the applications (see [7]). The use of C^1 elements gives good results, but the main drawbacks are the complexity of the elements and the poor stability for irregular solution. A second type of approximation, so-called non conforming approximation, is based on the idea of relaxing the continuity of functions and of their normal derivatives along the boundaries of elements. The most well-known elements in this class is the discrete Kirchhoff triangle DKT (discrete Kirchhoff triangle) which was used in [4] to approximate a Koiter model. Numerical locking is a serious drawback for this element when considering bending-dominated shells with very small thickness.

A new formulation was introduced in [7]; it is based on the idea of using a local basis-free formulation in which the unknowns are described in Cartesian coordinates. This new formulation allows to handle shells with a $W^{2,\infty}$-middle surface. Its approximation by finite element methods was considered in [6] and implemented using the finite element software Freefem++ [17]. This new formulation enters in the family of problems where the constraint is distributed over the domain, like the divergence-free constraint for incompressible Stokes flows.

Penalty methods are already efficiently used to handle constrained problems (see [20]). Roughly speaking, a penalty method consists in adding an extra term, the penalty term $p^{-1}b(u,v)$[3], to the variational formulation in order to handle the constraint. In [3] a penalty approach was used to prescribe non-homogeneous Dirichlet boundary conditions on the boundary. Recently, in the finite element context, some interesting contributions of the penalty method were presented in [23] where the author is also interested to geometrical constraints, namely interested in solving an elliptic problem on a simply shaped domain with holes. He highlights the difference between two kinds of penalty problems; closed and non closed penalty problems, *i.e.*, the case when $b(u,v) = (Bu, Bv)$ with B a linear operator with closed range or not. At the continuous level, the closed penalty problem was proved to be more accurate. In the same spirit, we reformulate Koiter's equation in Cartesian coordinates with a "closed penalization". Note that a non-closed penalization was already considered in [6]. We intend to show that the corresponding finite element method converges in the energy norm uniformly with respect to the mesh size and to the penalized parameter.

This paper is organized as follow: in Section 2, we first briefly recall the geometry of the surface as well as Koiter's shell model formulated in Cartesian coordinates and we point out the main difficulty for which the original problem can not be implemented in a conforming way. In Section 3 we introduce a penalized formulation of Koiter's model in which a new functional space and a new bilinear form are introduced. We prove that the penalized problem is well-posed. We present in Section 4 its finite element discretization and prove its well-posedness and its consistency. Hence the convergence of the method depend on its stability, which involves boundedness and coercivity of the bilinear form. As a result, for this problem, error estimates cannot be uniform in p. In Section 5 we introduce a new formulation for which we are able to show that the method converges uniformly with respect to the penalized parameter and the mesh size. Finally, we present some numerical tests in Section 6 that validate and illustrate our approach.

In the whole paper, the notation $a \lesssim b$ is used for the estimate $a \leq c\, b$, where c is a generic constant that does not depend on any mesh-size or penalized parameter. The convention of summation of repeated indices, which run from 1 to 2 when they are Greek is used.

2. The linear Koiter model for elastic shells

2.1. The continuous problem

Let (e_1, e_2, e_3) be the canonical orthogonal basis of $\mathbb{R}^3$, $u \cdot v$ the inner product of $\mathbb{R}^3$, $u \times v$ the vector product of u and v. For a given domain ω of $\mathbb{R}^2$ with a $C^{1,1}$ boundary, we consider a shell whose middle surface S is

[3]The parameter p is $0 < p < 1$ and is supposed to tend to zero.

given by

$$S = \varphi(\bar{\omega}) \text{ where } \varphi \in W^{2,\infty}(\omega, \mathbb{R}^3) \tag{2.1}$$

where $W^{m,p}$ denotes the usual Sobolev space. φ is supposed to be a one-to-one mapping such that the two vectors[4]

$$a_\alpha = \partial_\alpha \varphi, \ \alpha = 1, 2 \tag{2.2}$$

are linearly independent. The normal vector a_3 is given by

$$a_3 = \frac{a_1 \times a_2}{|a_1 \times a_2|}. \tag{2.3}$$

The contravariant basis a^i is defined by the relation

$$a_i \cdot a^j = \delta_i^j, \quad \delta_i^j \text{ being the Kronecker symbol.} \tag{2.4}$$

The covariant and contravariant components of the metric (or the fist fundamental form) are given by:

$$(a_{\alpha\beta}) = (a_\alpha \cdot a_\beta) \text{ and } (a^{\alpha\beta}) = (a_{\alpha\beta})^{-1}, a = \det(a_{\alpha\beta}). \tag{2.5}$$

$\sqrt{a}$ is the area element of the midsurface in the chart. The length element ℓ on the boundary $\partial\omega$ is given by $\sqrt{a^{\alpha\beta}\tau_\alpha\tau_\beta}$, (τ_1, τ_2) being the covariant coordinates of a unit vector tangent to $\partial\omega$.

The second fundamental form of the surface is given in covariant components by

$$b_{\alpha\beta} = a_3 \cdot \partial_\beta a_\alpha = -a_\alpha \cdot \partial_\beta a_3. \tag{2.6}$$

The Christoffel symbols of the surface $\Gamma^\gamma_{\alpha\beta}$ take the form

$$\Gamma^\gamma_{\alpha\beta} = \Gamma^\gamma_{\beta\alpha} = a^\gamma \cdot \partial_\beta a_\alpha = a^\gamma \cdot \partial_\alpha a_\beta. \tag{2.7}$$

We consider here the case of a homogeneous, isotropic material with Young modulus $E > 0$ and Poisson ratio ν, $0 \leq \nu < \frac{1}{2}$. We also denote by ε the thickness of the shell which is assumed to be constant and positive.

Let $a^{\alpha\beta\rho\sigma}$ denote the contravariant components of the elasticity tensor, its components are given by

$$a^{\alpha\beta\rho\sigma} = \frac{E}{2(1+\nu)}(a^{\alpha\rho}a^{\beta\sigma} + a^{\alpha\sigma}a^{\beta\rho}) + \frac{E\nu}{2(1-\nu^2)}a^{\alpha\beta}a^{\rho\sigma}. \tag{2.8}$$

We note that the Assumption (2.1) on the chart is made such that each component of the elasticity tensor belongs to $W^{1,\infty}$. Moreover, this tensor satisfies the usual symmetry properties and is uniformly strictly positive *i.e.*, there exists a positive constant c_0 such that

$$a^{\alpha\beta\rho\sigma}\tau_{\alpha\beta}\tau_{\rho\sigma} \geq c_0|\tau|^2 \ \text{ a.e. in } \omega, \forall \tau, \text{ symmetric tensor of order 2.} \tag{2.9}$$

Let $u \in H^1(\omega, \mathbb{R}^3)$ be the middle surface displacement. Following [7], the covariant components of the change of metric tensor and the covariant components of the change of curvature tensor are respectively defined by

$$\gamma_{\alpha\beta}(u) = \frac{1}{2}(\partial_\alpha u \cdot a_\beta + \partial_\beta u \cdot a_\alpha), \tag{2.10}$$

$$\Upsilon_{\alpha\beta}(u) = \left(\partial_{\alpha\beta} u - \Gamma^\rho_{\alpha\beta}\partial_\rho u\right) \cdot a_3 \ . \tag{2.11}$$

We finally introduce respectively the stress resultant and the stress couple

$$n^{\alpha\beta}(u) = \varepsilon a^{\alpha\beta\rho\sigma}\gamma_{\alpha\beta}(u), \tag{2.12}$$

$$m^{\alpha\beta}(u) = \frac{\varepsilon^3}{12}a^{\alpha\beta\rho\sigma}\Upsilon_{\alpha\beta}(u). \tag{2.13}$$

[4]For simplicity, here and below, we omit x in the previous notations $a_\alpha(x), a_3(x), \ldots$

2.2. The variational formulation for a totally clamped shell

The functional space for Koiter's solution is $H^1(\omega) \times H^1(\omega) \times H^2(\omega)$, when the classical formulation is used and the totally clamping condition reads

$$u_i = \partial_\nu u_3 = 0, \quad \text{on } \partial\omega \tag{2.14}$$

where ∂_ν denotes the normal derivative on the boundary. Blouza and Le Dret in [7], rewrite the condition (2.14) in a simpler and more intrinsic fashion that makes sense in the context of shells with little regularity; the new clamping condition reads[5]

$$u = 0 \text{ on } \partial\omega \quad \text{and} \quad \partial_\alpha u \cdot a_3 = 0 \text{ in } H^{1/2}(\partial\omega). \tag{2.15}$$

Therefor, the functional space $\mathbb{V}(\omega)$, which is appropriate for shell with little regularity, reads

$$\mathbb{V}(\omega) = \left\{ v \in H_0^1\left(\omega, \mathbb{R}^3\right), \partial_\alpha v \cdot a_3 \in H_0^1(\omega) \right\}, \tag{2.16}$$

equipped with the norm:

$$\|v\|_{\mathbb{V}(\omega)} = \left(\|v\|^2_{H^1(\omega,\mathbb{R}^3)} + \|\partial_\alpha v \cdot a_3\|^2_{H^1(\omega)} \right)^{\frac{1}{2}}. \tag{2.17}$$

The variational formulation of the problem corresponding to the linear Koiter model for shells with little regularity reads:

$$\begin{cases} \text{Find } u \in \mathbb{V}(\omega) \text{ such that} \\ \mathbf{a}(u, v) = \mathcal{L}(v), \forall v \in \mathbb{V}(\omega), \end{cases} \tag{2.18}$$

where,

$$\mathbf{a}(u, v) = \int_\omega \left(n^{\rho\sigma}(u) \gamma_{\rho\sigma}(v) + m^{\rho\sigma}(u) \Upsilon_{\rho\sigma}(v) \right) \sqrt{a} \mathrm{d}x, \tag{2.19}$$

$$\mathcal{L}(v) = \int_\omega f \cdot v \sqrt{a} \mathrm{d}x. \tag{2.20}$$

Theorem 2.1 [7]. *Let $f \in L^2(\omega, \mathbb{R}^3)$ be a given force resultant density. Then the variational problem (2.18) has a unique solution in $\mathbb{V}(\omega)$.*

Recently, a more realistic formulation was proposed by considering the terms $\partial_\alpha u \cdot a_3$ as independent unknowns say r_α. Then it is clear that, if $s_\alpha := \partial_\alpha v \cdot a_3$, the vector $s := s_\alpha a^\alpha$ belongs to the space $H_0^1(\omega, \mathbb{R}^3)$ provided that v belongs to $\mathbb{V}(\omega)$. A straightforward calculus amounts to rewrite the new change of curvature tensor and the stress couple as follows:

$$\Upsilon_{\alpha\beta}(u) := \chi_{\alpha\beta}(u, r) := \frac{1}{2}\left(\partial_\alpha u \cdot \partial_\beta a_3 + \partial_\beta u \cdot \partial_\alpha a_3\right) + \frac{1}{2}\left(\partial_\alpha r \cdot a_\beta + \partial_\beta r \cdot a_\alpha\right), \tag{2.21}$$

$$:= \theta_{\alpha\beta}(u) + \gamma_{\alpha\beta}(r) \tag{2.22}$$

$$m^{\alpha\beta}(u) := m^{\alpha\beta}(u, r) := \frac{\varepsilon^3}{12} a^{\alpha\beta\rho\sigma} \chi_{\alpha\beta}(u, r) \tag{2.23}$$

and to reformulate the problem (2.18) as follows:

$$\begin{cases} \text{Find } U = (u, r) \in \mathbb{W}(\omega) \text{ such that} \\ \mathbf{a}((u, r); (v, s)) = \mathcal{L}((v, s)), \forall V = (v, s) \in \mathbb{W}(\omega), \end{cases} \tag{2.24}$$

[5]The condition (2.15) coincides with the classical clamping condition for φ smooth.

where,

$$\mathbb{W}(\omega) = \left\{(v,s) \in (H_0^1(\omega,\mathbb{R}^3))^2 \mid \quad s + (\partial_\alpha v \cdot a_3)a^\alpha = 0 \text{ a.e in } \omega\right\}, \tag{2.25}$$

$$\mathbf{a}((u,r);(v,s)) = \int_\omega \left(n^{\rho\sigma}(u)\gamma_{\rho\sigma}(v) + m^{\rho\sigma}(U)\chi_{\rho\sigma}(V)\right)\sqrt{a}\mathrm{d}x, \tag{2.26}$$

$$\mathcal{L}((v,s)) = \int_\omega f \cdot v\sqrt{a}\mathrm{d}x. \tag{2.27}$$

Remark 2.2. Note that, if $(v,s) \in \mathbb{W}(\omega)$ the constraint

$$s + (\partial_\alpha v \cdot a_3)a^\alpha = 0 \quad \text{a.e, in } \omega, \tag{2.28}$$

or

$$s \cdot a_\alpha + (\partial_\alpha v \cdot a_3) = 0 \quad \text{a.e, in } \omega, \quad \alpha = 1,2 \tag{2.29}$$

cannot be implemented in a standard conforming way (see [6]). This amounts to say that the problem (2.24) cannot be approximated by conforming methods for a general shell.

3. A penalized version

According to Remark 2.2, in order to avoid the constraint (2.28), as alternative approach we propose to introduce a penalized version of (2.24). This means that we reformulate the original constrained problem as an unconstrained one.

Let us consider the functional space:

$$\mathbb{X}(\omega) = \{(v,s) \in H_0^1(\omega,\mathbb{R}^3) \times H_0^1(\omega,\mathbb{R}^3), \partial_\alpha v \cdot a_3 \in H_0^1(\omega)\} \tag{3.1}$$

equipped with the norm

$$\|(v,s)\|_{\mathbb{X}(\omega)} = \left(\|v\|^2_{H^1(\omega,\mathbb{R}^3)} + \|s\|^2_{H^1(\omega,\mathbb{R}^3)} + \|\partial_\alpha v \cdot a_3\|^2_{H^1(\omega)}\right)^{\frac{1}{2}}. \tag{3.2}$$

Clearly, equipped with this norm, $\mathbb{X}(\omega)$ is a Hilbert space.

Let $p \in \mathbb{R}, 0 < p \leq 1$. We consider the following variational problem:

$$\begin{cases} \text{Find } U_p = (u_p, r_p) \in \mathbb{X}(\omega) \text{ such that} \\ \mathbf{a}(U_p, V) + (1+p^{-1})b(U_p, V) = \mathcal{L}(V), \forall V \in \mathbb{X}(\omega). \end{cases} \tag{3.3}$$

For $W = (w,t), V = (v,s) \in \mathbb{X}(\omega)$, the bilinear form $b(\cdot,\cdot)$ reads

$$b(W,V) = \int_\omega \nabla(t + (\partial_\alpha w \cdot a_3)a^\alpha) : \nabla(s + (\partial_\alpha v \cdot a_3)a^\alpha)\mathrm{d}x \tag{3.4}$$

Here, for $v = (v_1, v_2, v_3) \in H^1(\omega,\mathbb{R}^3)$, we have set

$$\nabla v = \begin{pmatrix} \partial_1 v_1 & \partial_2 v_1 \\ \partial_1 v_2 & \partial_2 v_2 \\ \partial_1 v_3 & \partial_2 v_3 \end{pmatrix} \text{ and } A : B = \sum_{\alpha,j} A_{\alpha j} B_{\alpha j} = tr(AB^T)$$

Note that the space $H_0^1(\omega,\mathbb{R}^3)$ has the inner product:

$$(u,v)_{H_0^1(\omega,\mathbb{R}^3)} = \int_\omega \nabla u : \nabla v \ \mathrm{d}x = \sum_i \int_\omega \nabla u_i \cdot \nabla v_i \ \mathrm{d}x = \sum_{\alpha,j} \int_\omega \partial_\alpha u_j \partial_\alpha v_j \ \mathrm{d}x$$

Remark 3.1. Alternatively, we could consider the following bilinear form:

$$\bar{b}(W,V)=\int_{\omega}(t+(\partial_\alpha w\cdot a_3)a^\alpha)\cdot(s+(\partial_\alpha v\cdot a_3)a^\alpha)\mathrm{d}x, \tag{3.5}$$

instead of b. At the continuous level, the difference between choosing (3.4) and (3.5) lies on the fact that the use of $\bar{b}(\cdot,\cdot)$ leads to an error of order $\sqrt{p}$ between the original solution and the penalized one (see [6,23]). Whereas, the choice (3.4) gives an error of order p.

Lemma 3.2. *The bilinear form* $\mathbf{a}+b$ *is* $\mathbb{X}(\omega)$*-elliptic.*

Proof. The proof is quite similar to that of ([7], Lem. 11), for the sake of completeness, let us give the proof by a contradiction argument. Indeed if $\mathbf{a}+b$ is not $\mathbb{X}(\omega)$-elliptic, then there exists a sequence of $(V_n)_{n\in\mathbb{N}}=((v_n,s_n))_{n\in\mathbb{N}}$ with $V_n\in\mathbb{X}(\omega)$, for all $n\in\mathbb{N}$ such that

$$\|V_n\|_{\mathbb{X}(\omega)}=1,\forall n\in\mathbb{N},\quad\text{and}\quad\mathbf{a}(V_n,V_n)+b(V_n,V_n)\to 0\qquad\text{as}\qquad n\to+\infty. \tag{3.6}$$

Then, by extracting a subsequence, still denoted $(V_n)_{n\in\mathbb{N}}$, there exists a $V\in\mathbb{X}(\omega)$ such that $V_n\rightharpoonup V$ weakly in $\mathbb{X}(\omega)$ and $\mathbf{a}(V,V)+b(V,V)=0$. This means that $V\in\mathbb{W}(\omega)$ and $\mathbf{a}(V,V)=0$. Then the rigid movement lemma (see [7]) implies that $V=0$.

Hence, $v_n\rightharpoonup 0$, $s_n\rightharpoonup 0$ weakly in $H^1(\omega,\mathbb{R}^3)$ and $\partial_\alpha v_n\cdot a_3\rightharpoonup 0$ weakly in $H^1(\omega)$.

Let $w_n=(v_n\cdot a_1,v_n\cdot a_2)$ then we have

$$2e_{\alpha\beta}(w_n)=2\gamma_{\alpha\beta}(w_n)+v_n\cdot(\partial_\alpha a_\beta+\partial_\beta a_\alpha)\to 0\qquad\text{in}\qquad L^2(\omega).$$

By the two dimensional version of Korn's inequality $w_n\to 0$ in $H^1(\omega)$ and therefore $\partial_\alpha(v_n\cdot a_\beta)\to 0$ in $L^2(\omega)$. This property, the identity $\partial_\alpha(v_n\cdot a_\beta)=\partial_\alpha v_n\cdot a_\beta+v_n\cdot\partial_\alpha a_\beta$ and the weak convergence of v_n to 0 in $H^1(\omega,\mathbb{R}^3)$ imply, up to a subsequence, that $\partial_\alpha v_n\cdot a_\beta\to 0\quad$ in $L^2(\omega)$.

Since $\partial_\alpha v_n\cdot a_3\rightharpoonup 0$ weakly in $H^1(\omega)$, again up to a subsequence, it convergences strongly in $L^2(\omega)$, and by the previous property, we get

$$v_n\to 0\text{ strongly in }H^1(\omega,\mathbb{R}^3). \tag{3.7}$$

We have also

$$\|\gamma_{\alpha\beta}(s_n)+\theta_{\alpha\beta}(v_n)\|_{L^2(\omega)}\to 0\qquad\text{as}\quad n\to+\infty$$

together with $\|\theta_{\alpha\beta}(v_n)\|_{L^2(\omega)}\le\|v_n\|_{H^1(\omega,\mathbb{R}^3)}\to 0$, we deduce that

$$\theta_{\alpha\beta}(v_n)\to 0\text{ and }\gamma_{\alpha\beta}(s_n)\to 0\qquad\text{in}\quad L^2(\omega).$$

Now let $t_n=(s_n\cdot a_1,s_n\cdot a_2)$ then a simple calculation gives

$$2e_{\alpha\beta}(t_n)=2\gamma_{\alpha\beta}(s_n)+s_n\cdot(\partial_\alpha a_\beta+\partial_\beta a_\alpha)\to 0\quad\text{in}\quad L^2(\omega)\quad\text{as }n\to+\infty.$$

By two dimensional Korn's inequality

$$t_n\to 0\text{ in }H^1(\omega)\Longrightarrow\partial_\alpha(t_n\cdot a_\beta)\to 0\quad\text{in}\quad L^2(\omega),$$

thus,

$$\partial_\alpha(s_n\cdot a_\beta)\to 0\text{ and }s_n\cdot a_\beta\to 0\quad\text{strongly in }H^1(\omega). \tag{3.8}$$

In addition we have

$$\|s_n+(\partial_\alpha v_n\cdot a_3)a^\alpha\|_{H^1(\omega,\mathbb{R}^3)}\to 0\quad\text{and}\quad s_n\cdot a_\alpha\to 0\text{ strongly in }H^1(\omega).$$

Hence,

$$\partial_\alpha v_n\cdot a_3\to 0\text{ strongly in }H^1(\omega)\qquad\text{as}\quad n\to+\infty.$$

This last property, combined with (3.7) and (3.8) lead to contradiction with the first properties of (3.6). □

Theorem 3.3. *Let $f \in L^2(\omega, \mathbb{R}^3)$. Then the problem (3.3) has a unique solution.*

Proof. Apply the Lax−Milgram lemma. □

Now we need to prove that the penalized problem provides an approximation of the constrained problem. Let $\Lambda = H_0^1(\omega, \mathbb{R}^3)$ and define the operator B by

$$B : \mathbb{X}(\omega) \to \Lambda : V = (v, s) \mapsto B(v, s) = s + (\partial_\alpha v \cdot a_3)a^\alpha.$$

Then clearly

$$b((w, t); (v, s)) = (B(w, t), B(v, s))_\Lambda .$$

Proposition 3.4. *The operator B is surjective.*

Proof. It is clear that B is a linear bounded operator. Indeed,

$$\|B(v, s)\|_\Lambda = \|s + (\partial_\alpha v \cdot a_3)a^\alpha\|_\Lambda \lesssim \|(v, s)\|_{\mathbb{X}(\omega)}$$

Let

$$B^* : H^{-1}(\omega, \mathbb{R}^3) \mapsto (\mathbb{X}(\omega))^*$$

be the adjoint operator of B then

$$\|B^*\varphi\|_{(\mathbb{X}(\omega))^*} = \sup_{(v,s)\neq 0} \frac{|\langle B^*\varphi, (v, s)\rangle|}{\|(v, s)\|_{\mathbb{X}(\omega)}} = \sup_{(v,s)\neq 0} \frac{|\langle \varphi, B(v, s)\rangle|}{\|(v, s)\|_{\mathbb{X}(\omega)}} \gtrsim \frac{|\langle \varphi, y\rangle|}{\|y\|_{H^1(\omega)}},$$

where we have chosen $(v, s) = (0, y)$, with $y \in \Lambda$ satisfies $\langle \varphi, v\rangle = (y, v)_{H^1}, \forall v \in \Lambda$ and $\|\varphi\|_{H^{-1}} = \|y\|_{H_0^1}$.

This directly implies that

$$\|B^*\varphi\|_{(\mathbb{X}(\omega))^*} \gtrsim \|\varphi\|_{\Lambda^*}, \quad \forall \varphi \in \Lambda^*. \tag{3.9}$$

By the open mapping theorem and the closed range theorem (see [12], Thm. 2.20 for instance), we deduce that B is surjective. □

Following to Maury ([23], Cor. 2.4), we have the following estimates.

Corollary 3.5. *Let $U = (u, r)$ and $U_p = (u_p, r_p)$ respectively, be the unique solutions of problems (2.24) and (3.3). Then*

$$\|r_p + (\partial_\alpha u_p \cdot a_3)a^\alpha\|_{H_0^1(\omega,\mathbb{R}^3)} \lesssim p\|f\|_{L^2(\omega,\mathbb{R}^3)}. \tag{3.10}$$

$$\|U_p - U\|_{\mathbb{X}(\omega)} \lesssim p\|f\|_{L^2(\omega,\mathbb{R}^3)}. \tag{3.11}$$

It is readily checked that the variational problem (3.3) is equivalent to the following boundary values problem:

$$\begin{cases} -\partial_\rho((n^{\rho\sigma}(u_p)a_\sigma + m^{\rho\sigma}(U_p)\partial_\sigma a_3)\sqrt{a}) + (1 + p^{-1})\partial_\rho\left((\Delta(r_p + (\partial_\sigma u_p \cdot a_3)a^\sigma) \cdot a^\rho)a_3\right) = f\sqrt{a} & \text{in} \quad \omega, \\ -\partial_\rho(m^{\rho\sigma}(U_p)a_\sigma\sqrt{a}) - (1 + p^{-1})\Delta(r_p + (\partial_\sigma u_p \cdot a_3)a^\sigma) = 0 & \text{in} \quad \omega, \\ u_p = r_p = 0 & \text{on} \quad \partial\omega. \end{cases} \tag{3.12}$$

When the bilinear form $b(\cdot, \cdot)$ is replaced by $\bar{b}(\cdot, \cdot)$ defined in (3.5), we notice that the corresponding system is an elliptic system of linear second-order partial differential equations. However, in their classical formulation (see [15]), Koiter's equations for a linearly elastic shell are made of a linear fourth-order partial differential equation for the normal component $u \cdot a_3$ and two linear second-order partial differential equations for the tangential components as it is the case for system (3.12).

The next section is devoted to the discretization of the problem (3.3) by a finite element method.

4. Approximation by finite elements of the penalized problem (3.3)

Let $(\mathcal{T}_h)_{h>0}$ be a regular affine family of triangulations which covers the domain ω. Let $\mathcal{E}_h$ be the set of (open) edges in $\mathcal{T}_h, \mathcal{E}_h^i$ and $\mathcal{E}_h^b$ the set of interior and boundary edges. $\mathcal{N}_h$ the set of all nodes. We introduce the finite dimensional spaces

$$\mathbb{X}_h = \{V_h = (v_h, s_h) \in (C^0(\bar{\omega})^3)^2 / V_{h|T} \in (\mathbb{P}_k(T)^3)^2,\ \forall T \in \mathcal{T}_h, k \geq 2, V_h|_{\partial\Omega} = 0\}. \tag{4.1}$$

For $e \in \mathcal{E}_h$ and s a piecewise H^2 vector, we define the jump $[[s]]$ of s across e and its average $[[s]]$ on e as follows. If $e \subset \omega$, we choose $\underline{\nu}^e = (\nu_1, \nu_2)$ to be one of the two unit vector normal to e. Then e is the common side of $T_\pm \in \mathcal{T}_h$, where $\underline{\nu} = \underline{\nu}^{e+}$ is pointing from T_+ to T_-.

$$[[s]] = s^+ - s^-, \tag{4.2}$$

If $e \subset \partial\omega$, we simply take $[[s]] = s$.

Then we consider the following discrete problem:

$$\begin{cases} \text{Find } U_{p,h} = (u_{p,h}, r_{p,h}) \in \mathbb{X}_h \text{ such that} \\ \mathcal{A}(U_{p,h}, V_h) + p^{-1}\tilde{b}(U_{p,h}, V_h) = \mathcal{L}(V_h), \forall V_h = (v_h, s_h) \in \mathbb{X}_h, \end{cases} \tag{4.3}$$

where

$$\mathcal{A}(U_h, V_h) = \tilde{a}(U_h, V_h) + \tilde{b}(U_h, V_h) + d(U_h, V_h),$$

and the bilinear forms $\tilde{a}(.,.)$ and $\tilde{b}(.,.)$ are given by

$$\tilde{a}(U_h, V_h) = \sum_{T \in \mathcal{T}_h} \int_T \left(n^{\rho\sigma}(u_h)\gamma_{\rho\sigma}(v_h) + m^{\rho\sigma}(U_h)\chi_{\rho\sigma}(V_h)\right)\sqrt{a}\mathrm{d}x$$

$$\tilde{b}(U_h, V_h) = \sum_{T \in \mathcal{T}_h} \int_T \nabla(r_h + (\partial_\alpha u_h \cdot a_3)a^\alpha) : \nabla(s_h + (\partial_\alpha v_h \cdot a_3)a^\alpha)\ \mathrm{d}x,$$

Furthermore, we take

$$d(U_h, V_h) = \sum_{e \in \mathcal{E}_h} \int_e [[(\partial_\alpha u_h \cdot a_3)a^\alpha]] \cdot [[(\partial_\alpha v_h \cdot a_3)a^\alpha]]\ de.$$

4.0.1. Mesh-dependent norms

Let us define the following quantities: for $(v_h, s_h) \in \mathbb{X}_h$, we set

$$\| (v_h, s_h) \|_h^2 = \sum_{T \in \mathcal{T}_h} \left(\sum_{\alpha\beta} \left(\|\gamma_{\alpha\beta}(v_h)\|_{0,T}^2 + \|\chi_{\alpha\beta}(v_h, s_h)\|_{0,T}^2 \right) \right. \tag{4.4}$$

$$\left. + \sum_{T \in \mathcal{T}_h} \left(\|\nabla(s_h + (\partial_\alpha v_h \cdot a_3)a^\alpha)\|_{(L^2(T))^{3\times 2}}^2 \right) \right.$$

$$\left. + \sum_{e \in \mathcal{E}_h} \left(\|[[(\partial_\alpha v_h \cdot a_3)a^\alpha]]\|_{(L^2(e))^3}^2 \right) . \right. \tag{4.5}$$

Proposition 4.1. *$\|\cdot\|_h$ defines a norm on the space $\mathbb{X}_h$ given by (4.1).*

Proof. Let $V=(v,s)\in\mathbb{X}_h$. Then $\|V\|_h=0$ if and only if

$$\sum_{\alpha\beta}\sum_{T\in\mathcal{T}_h}\left(\|\gamma_{\alpha\beta}(v)\|^2_{L^2(T)}+\|\chi_{\alpha\beta}(v,s)\|^2_{L^2(T)}\right)=0, \tag{4.6}$$

$$\sum_{e\in\mathcal{E}_h}\left(\|[[(\partial_\alpha v\cdot a_3)a^\alpha]]\|^2_{L^2(e)^3}\right)=0, \tag{4.7}$$

$$\sum_{T\in\mathcal{T}_h}\|\left(\nabla(s+\partial_\alpha v\cdot a_3)a^\alpha\right)\|^2_{L^2(T)^3}=0. \tag{4.8}$$

Equation (4.7) immediately implies that: $(\partial_\alpha v\cdot a_3)a^\alpha$ is continuous and it vanishes on $\partial\omega$, equation (4.8) and Poincaré's inequality imply that $s+(\partial_\alpha v\cdot a_3)a^\alpha=0$. Hence

$$(v,s)\in\mathbb{W}(\omega).$$

Then equation (4.6) means that $\mathbf{a}((v,s);(v,s))=0$. Hence (v,s) must be identically zero since $\mathbf{a}(\cdot\ ;\ \cdot)$ is $\mathbb{W}(\omega)$-elliptic (see [7], Lem. 11). □

Proposition 4.2. *The bilinear form $\mathcal{A}(.,.)+p^{-1}\tilde{b}(.,.)$ is continuous and coercive on $\mathbb{X}_h$.*

Proof. Let $V=(v,s)$ and $W=(w,t)\in\mathbb{X}_h$. Then by the Cauchy−Schwarz inequality we have:

$$\left|\mathcal{A}(V,W)+p^{-1}b(V,W)\right|\lesssim p^{-1}\|V\|_h\|W\|_h.$$

For the coercivity we have

$$\mathcal{A}(V,V)+p^{-1}b(V,V)\geq\mathcal{A}(V,V)$$

and therefore

$$\mathcal{A}(V,V)+p^{-1}b(V,V)\geq||(v,s)||_h^2. \tag{4.9}$$

Hence, the bilinear form $\mathcal{A}(.,.)+p^{-1}\tilde{b}(.,.)$ is uniformly $\mathbb{X}_h$-elliptic. □

5. *A priori* error analysis for the penalized problem (3.3)

Note that $\mathbb{X}_h\nsubseteq\mathbb{X}(\omega)$ because $\partial_\alpha u_h\cdot a_3\notin H^1_0(\Omega)$. But for any $V_p=(v_p,s_p)\in\mathbb{X}(\omega)$ we have

$$d(V_p,W)=0,\forall W\in\mathbb{X}(\omega)\cup\mathbb{X}_h.$$

Hence, the scheme (4.3) is *consistent* in the sense that .

$$\mathcal{A}(U_p,V_h)+p^{-1}\tilde{b}(U_p,V_h)=\mathcal{L}(V_h),\forall V_h\in\mathbb{X}_h. \tag{5.1}$$

Recalling that the solution $U_{p,h}\in\mathbb{X}_h$ of (4.3) satisfies

$$\mathcal{A}(U_{p,h},V_h)+p^{-1}\tilde{b}(U_{p,h},V_h)=\mathcal{L}(V_h),\forall V_h\in\mathbb{X}_h. \tag{5.2}$$

This allows to deduce the next error estimate.

Theorem 5.1. *Let U_p be the solution of problem (3.3) and $U_{p,h}$ the solution of problem (4.3). Then*

$$\|U_p-U_{p,h}\|_h\lesssim(1+p^{-1})\inf_{V_h\in\mathbb{X}_h}\|U_p-V_h\|_h \tag{5.3}$$

Proof. We recall that the continuity constant of the bilinear form $\mathcal{A}(.,.) + p^{-1}b(.,.)$ behaves like p^{-1} and coercivity constant like 1. Then we have:

$$\begin{aligned}\|U_p - U_{p,h}\|_h &\leq \|U_p - V_h\|_h + \|V_h - U_{p,h}\|_h \\ &\leq \|U_p - V_h\|_h + \sup_{W_h \in \mathbb{X}_h} \frac{\mathcal{A}(V_h - U_{p,h}, W_h) + p^{-1}b(V_h - U_{p,h}, W_h)}{\|W_h\|_h} \\ &= \|U_p - V_h\|_h + \sup_{W_h \in \mathbb{X}_h} \frac{\mathcal{A}(V_h - U_p, W_h) + p^{-1}b(V_h - U_p, W_h)}{\|W_h\|_h} \\ &\lesssim (1 + p^{-1})\|U_p - V_h\|_h, \quad \text{for any } V_h \in \mathbb{X}_h. \end{aligned}$$

□

Remark 5.2. Notice that the estimate provided for $\|U_p - U_{p,h}\|$ in Theorem 5.1 is not uniform in p. Hence for the scheme (4.3), the determination of the "best" parameter $1/p$ is typically performed experimentally. An alternative is to use a very fine mesh that is sufficient to deduce the optimal error estimate as long as h/p is uniformly bounded.

To obtain uniform estimate, we use a mixed formulation of problem (3.3). Let us first introduce the following quantity

$$\psi_p = \frac{B(U_p)}{p},$$

and rewrite the continuous penalized problem (3.3) as

$$\begin{cases} \text{Find } U_p = (u_p, r_p) \in \mathbb{X}(\omega) \text{ such that} \\ \mathcal{A}(U_p, V) + (\psi_p, B(V))_\Lambda = \mathcal{L}(V), \forall V = (v, s) \in \mathbb{X}(\omega), \\ (B(U_p), \phi)_\Lambda - p(\psi_p, \phi)_\Lambda = 0, \forall \phi \in \Lambda \end{cases} \tag{5.4}$$

Now we consider the following discrete problem:

$$\begin{cases} \text{Find } U_h = ((u_h, r_h), \psi_h) \in \mathbb{X}_h \times \Lambda_h \text{ such that} \\ \mathcal{A}(U_h, V_h) + (\psi_h, B(V_h))_\Lambda = \mathcal{L}(V_h), \forall V_h = (v_h, s_h) \in \mathbb{X}_h, \\ (B(U_h), \phi_h)_\Lambda - p(\psi_h, \phi_h)_\Lambda = 0, \forall \phi_h \in \Lambda_h. \end{cases} \tag{5.5}$$

where

$$\Lambda_h = \{\phi_h \in C^0(\bar{\omega})^3 / \phi_{h|T} \in \mathbb{P}_k(T)^3, \ \forall T \in \mathcal{T}_h, \phi_h = 0 \quad \text{on} \quad \partial\omega\}, \tag{5.6}$$

Proposition 5.3. *The discrete problem (5.5) has a unique solution.*

Proof. The proof follows easily from the Lax−Milgram lemma applied to the bilinear form:

$$\mathcal{C} : ((U, \psi); (V, \phi)) \mapsto \mathcal{A}(U, V) + (\psi, B(V))_\Lambda - (B(U), \phi)_\Lambda + p(\psi, \phi)_\Lambda$$

that is positive definite, in the sense that

$$\mathcal{C}((V, \phi); (V, \phi)) = \mathcal{A}(V, V) + p(\phi, \phi)_\Lambda \geq \|V\|_h^2 + p\|\phi\|_\Lambda^2, \quad \forall (V, \phi) \in \mathbb{X}_h \times \Lambda_h. \tag{5.7}$$

So there exist a unique solution $(U_h, \psi_h) \in \mathbb{X}_h \times \Lambda_h$ to the following problem:

$$\begin{cases} \text{Find } U_h = ((u_h, r_h), \psi_h) \in \mathbb{X}_h \times \Lambda_h \text{ such that} \\ \quad \mathcal{C}((U_h, \psi_h); (V_h, \phi_h) = \mathcal{L}(V_h), \forall (V_h, \phi_h) \in \mathbb{X}_h \times \Lambda_h, \end{cases} \tag{5.8}$$

Take $V_h = 0$ (Resp. $\phi_h = 0$) in (5.8) we get the second equation in (5.5) (Resp. the first equation in (5.5)). Hence the problem (5.5) has a unique solution. □

5.1. *A priori* analysis of the problem (5.4)

Theorem 5.4. *Let (U_p, ψ_p) be the solution of (5.4) and let (U_h, ψ_h) be the solution of problem (5.5). Then we have the following error estimate*

$$\|U_p - U_h\|_h + \sqrt{p}\|\psi_p - \psi_h\|_\Lambda \lesssim (1+\sqrt{p})\left(\inf_{W_h\in\mathbb{X}_h}\frac{\|U_p - W_h\|_h}{\sqrt{p}} + \inf_{\varphi_h\in\Lambda_h}\|\psi_p - \varphi_h\|_\Lambda\right). \tag{5.9}$$

Proof. For any $W_h, V_h \in \mathbb{X}_h$ and $\varphi_h, \phi_h \in \Lambda_h$ we have

$$\begin{aligned}\mathcal{A}(U_h - W_h, V_h)+(\psi_h - \varphi_h, B(V_h))_\Lambda &= \mathcal{L}(V_h) - \mathcal{A}(W_h, V_h) - (\varphi_h, B(V_h))\\ &= \mathcal{A}(U_p, V_h) + (\psi_p, B(V_h))_\Lambda - \mathcal{A}(W_h, V_h) - (\varphi_h, B(V_h))_\Lambda\\ &= \mathcal{A}(U_p - W_h, V_h) + (\psi_p - \varphi_h, B(V_h))_\Lambda,\end{aligned} \tag{5.10}$$

and

$$(\phi_h, B(U_h - W_h))_\Lambda - p(\psi_h - \varphi_h, \phi_h)_\Lambda = (\phi_h, B(U_p - W_h))_\Lambda - p(\psi_p - \varphi_h, \phi_h)_\Lambda. \tag{5.11}$$

Take $V_h = U_h - W_h$ and $\phi_h = \psi_h - \varphi_h$ and subtracting (5.11) from (5.10), we get

$$\begin{aligned}\mathcal{A}(U_h - W_h, U_h - W_h) + p(\psi_h - \varphi_h, \psi_h - \varphi_h)_\Lambda = \mathcal{A}(U_p - W_h, U_h - W_h) + (\psi_p - \varphi_h, B(U_h - W_h))_\Lambda\\ - (\psi_h - \varphi_h, B(U_p - W_h))_\Lambda + p(\psi_p - \varphi_h, \psi_h - \varphi_h)_\Lambda.\end{aligned} \tag{5.12}$$

But we have,

$$\frac{\mathcal{A}(U_p - W_h, U_h - W_h) + (\psi_p - \varphi_h, B(U_h - W_h))_\Lambda}{\|U_h - W_h\|_h + \sqrt{p}\|\psi_h - \varphi_h\|_\Lambda} \lesssim \|U_p - W_h\|_h + \|\psi_p - \varphi_h\|_\Lambda \tag{5.13}$$

$$\frac{p(\psi_h - \varphi_h, \psi_p - \varphi_h)_\Lambda}{\|U_h - W_h\|_h + \sqrt{p}\|\psi_h - \varphi_h\|_\Lambda} \lesssim \sqrt{p}\|\psi_p - \varphi_h\|_\Lambda \tag{5.14}$$

$$\frac{(\psi_h - \varphi_h, B(U_p - W_h))_\Lambda}{\|U_h - W_h\|_h + \sqrt{p}\|\psi_h - \varphi_h\|_\Lambda} \lesssim \frac{\|U_p - W_h\|}{\sqrt{p}}. \tag{5.15}$$

Since (see (5.7)),

$$\|W_h - U_h\|_h^2 + p\|\varphi_h - \psi_h\|_\Lambda^2 \lesssim \mathcal{A}(U_h - W_h, U_h - W_h) + p(\psi_h - \varphi_h, \psi_h - \varphi_h)_\Lambda \tag{5.16}$$

then

$$\|W_h - U_h\|_h + \sqrt{p}\|\varphi_h - \psi_h\|_\Lambda \lesssim (1+\sqrt{p})\left(\frac{\|U_p - W_h\|}{\sqrt{p}} + \|\psi_p - \varphi_h\|\right)$$ □

Again, the estimate provided for $\|U_p - U_h\|_h$ and $\|\psi_p - \psi_h\|_\Lambda$ in Theorem 5.4 is not uniform in p. The next theorem gives a uniform estimate with respect to the penalized parameter p.

Theorem 5.5. *Let (U_p, ψ_p) the solution of (5.4) and let (U_h, ψ_h) the solution of problem (5.5). Then we have the following error estimate*

$$\|U_p - U_h\|_h + \sqrt{p}\|\psi_p - \psi_h\|_\Lambda \lesssim \inf_{W_h\in\mathbb{X}_h}\|U_p - W_h\|_h + \inf_{\varphi_h\in\Lambda_h}\|\psi_p - \varphi_h\|_\Lambda. \tag{5.17}$$

Proof. From (5.12) and Proposition 4.2 we observe that:

$$\mathcal{A}(U_h - W_h, U_h - W_h) + p(\psi_h - \varphi_h, \psi_h - \varphi_h)_\Lambda = \mathcal{A}(U_p - W_h, U_h - W_h) + (\psi_p - \varphi_h, B(U_h - W_h))_\Lambda - (\psi_h - \varphi_h, B(U_p - W_h))_\Lambda + p(\psi_p - \varphi_h, \psi_h - \varphi_h)_\Lambda \quad (5.18)$$

this gives,

$$\|W_h - U_h\|_h^2 + p\|\varphi_h - \psi_h\|_\Lambda^2 \le C_1(\|U_p - W_h\|_h\|U_h - W_h\|_h + \|U_h - W_h\|_h\|\psi_p - \varphi_h\|_\Lambda + \|U_p - W_h\|_h\|\psi_h - \varphi_h\|_\Lambda + p\|\psi_p - \varphi_h\|_\Lambda\|\psi_h - \varphi_h\|_\Lambda) \quad (5.19)$$

To obtain (5.17) we need to treat $\|U_p - W_h\|_h\|\psi_h - \varphi_h\|_\Lambda$ differently. Indeed, we have

$$\|\psi_h - \varphi_h\|_\Lambda \lesssim \sup_{V_h \in \mathbb{X}_h \setminus \{0\}} \frac{(\psi_h - \varphi_h, B(V_h))_\Lambda}{\|V_h\|_h} \quad (5.20)$$

which can be obtained by choosing $V_h = (0, \psi_h - \varphi_h)$ which implies that $B(V_h) = \psi_h - \varphi_h$ and that

$$\|V_h\|_h^2 = \sum_{T \in \mathcal{T}_h} \left(\sum_{\alpha\beta} \left(\|\gamma_{\alpha\beta}(\psi_h - \phi_h)\|_{0,T}^2 + \|\nabla(\psi_h - \phi_h)\|_{L^2(T)^{2\times 3}}^2 \right) \lesssim \|\psi_h - \phi_h\|_\Lambda^2. \right.$$

From (5.20) and (5.10) we infer

$$\|\psi_h - \varphi_h\|_\Lambda \lesssim \|U_p - W_h\|_h + \|\psi_p - \varphi_h\|_\Lambda + \|U_h - W_h\|_h.$$

This estimate in (5.19) yields

$$\|W_h - U_h\|_h^2 + p\|\varphi_h - \psi_h\|_\Lambda^2 \lesssim \|U_p - W_h\|_h\|U_h - W_h\|_h + \|U_h - W_h\|_h\|\psi_p - \varphi_h\|_\Lambda + \|U_p - W_h\|_h^2 + \|U_p - W_h\|_h\|\psi_p - \varphi_h\|_\Lambda + p\|\psi_p - \varphi_h\|_\Lambda\|\psi_h - \varphi_h\|_\Lambda.$$

The conclusion follows by using Young's inequality. □

Proposition 5.6. *Assume that the solution $U_p \in (H^2(\omega, \mathbb{R}^3))^2$. Then we have the following concrete estimate*:

$$\|U_p - U_h\|_h + \|\psi_p - \psi_h\|_\Lambda \lesssim h\|U_p\|_{(H^2(\omega,\mathbb{R}^3))^2} \quad (5.21)$$

for the solution U_h of (5.4).

Proof. Let Π_h be the Lagrange interpolation operator. We have the following standard interpolation error estimates (see [11,14]) $\forall T \in \mathcal{T}_h, \forall \xi \in H^2(\omega)$.

$$h_T^{-4}\|\xi - \Pi_h(\xi)\|_{L^2(T)}^2 + h_T^{-2}|\xi - \Pi_h(\xi)|_{H^1(T)}^2 + |\xi - \Pi_h(\xi)|_{H^2(T)}^2 \lesssim \|\xi\|_{H^2(T)}^2, \quad (5.22)$$

Note that if $U_p \in \mathbb{X}(\omega) \cap (H^2(\omega, \mathbb{R}^3))^2$ then using the second equation in (3.12), the elliptic regularity theory implies that $\psi_p \in \Lambda \cap H^2(\omega, \mathbb{R}^3)$ with the estimate

$$\|\psi_p\|_{H^2(\omega,\mathbb{R}^3)} \lesssim \frac{1}{p+1}\|\partial_\rho(m^{\rho\sigma}(U_p)a_\sigma\sqrt{a})\|_{L^2(\omega,\mathbb{R}^3)} \lesssim \|U_p\|_{H^2}.$$

Taking in (5.17), $(W_h, \varphi_h) = \Pi_h(U_p, \psi_p)$, the conclusion follows by using the previous estimates in (5.3). □

Similarly, we can state the next error estimate.

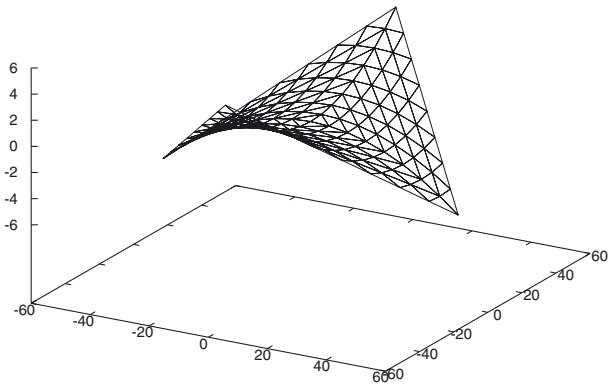

FIGURE 1. The surface $S = \varphi(\omega)$.

Proposition 5.7. *Assume that the solution U_p of problem (3.3) satisfies $U_p \in (H^s(\omega, \mathbb{R}^3))^2$, for some $s > 1$ and let U_h be the solution of (5.4). Then we have the following concrete estimate*:

$$\|U_p - U_h\|_h + \|\psi_p - \psi_h\|_\Lambda \lesssim h^{\gamma-1}\|U_p\|_{(H^s(\omega,\mathbb{R}^3))^2}, \tag{5.23}$$

where $\gamma = \min(s, k+1)$ and we recall that $k \geq 2$ is the order of the Lagrange finite element space $\mathbb{X}_h$.

Remark 5.8. From the previous proof we notice that to bound the error between U the solution of (2.24) and U_h the solution of (5.4) we have to add a term of order p to the right hand side due to the fact that:

$$\|U - U_h\|_h \leq \|U - U_p\|_h + \|U_p - U_h\|_h \lesssim p + \|U_p - U_h\|_h \tag{5.24}$$

6. Numerical experiments

In this section we have implemented two penalized versions of (4.3) (with b and $\bar{b}$) and the mixed formulation (5.4) using the finite element package FreeFem++ [17].

6.1. Hyperbolic paraboloid shell

We consider the hyperbolic paraboloid shell which is a literature benchmark for shell elements (see [4,5,8]). We intend to obtain reasonable results using the $P2$ Lagrange elements for all unknowns.

The reference domain ω is

$$\omega = \left\{(x, y) \in \mathbb{R}^2, \mid x \mid + \mid y \mid < 50\sqrt{2}\right\} \tag{6.1}$$

and the chart is defined by (see Fig. 1)

$$\varphi(x, y) = (x, y, K(x^2 - y^2)), \;\; K = 0.002. \tag{6.2}$$

The shell is clamped on $\partial\omega$ and subjected to a uniform pressure $q = 0.01$ kp/cm2.

As Young's modulus and Poisson's ratio we take $E = 2.85 \times 10^4$ kp/cm2, $\nu = 0.4$ respectively, while the thickness of the shell is $\varepsilon = 0.8$ cm. The reference value for this test is $u_3(0, 0)$. Its computed value by various continuous or discontinuous finite element methods is around -0.024313 cm (see [4,8]). Due to symmetry, only one quarter of the domain is modeled. The symmetry conditions are:

$$\begin{aligned} u_2 = r_2 = 0 \qquad &\text{on} \qquad y = 0, \\ u_1 = r_1 = 0 \qquad &\text{on} \qquad x = 0. \end{aligned}$$

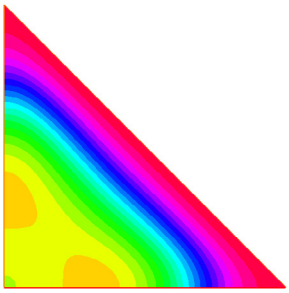

(A) isovalues for u_3, $p^{-1} = \dfrac{200E}{2(\nu+1)}$

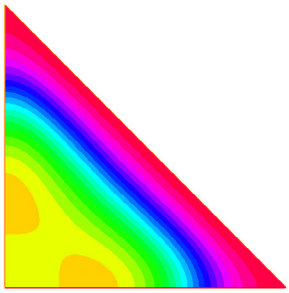

(B) isovalues for u_3, $p^{-1} = \dfrac{500E}{2(\nu+1)}$

FIGURE 2. Isovalues for u_3 using (4.3) with b.

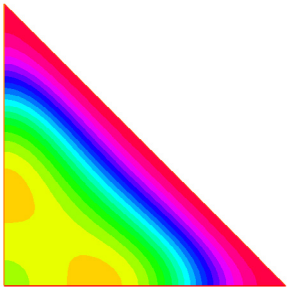

(A) Isovalues for u_3, $p^{-1} = \dfrac{E}{2(\nu+1)}$

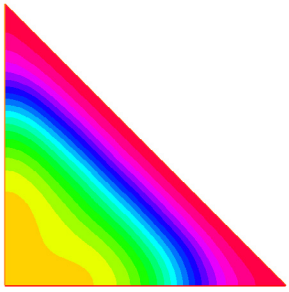

(B) Isovalues for u_3, $p^{-1} = \dfrac{500E}{2(\nu+1)}$

FIGURE 3. Isovalues for u_3 using (4.3) with $\bar{b}$.

TABLE 1. Error and constraint using (4.3).

p^{-1}	1e04	5e04	1e05	5e05	1e06	5e06
Err	0.000376788	9.57444e-06	6.35988e-05	0.000100536	0.000313105	0.000471888
Maximum value for the constraint	4.7024e-08	5.40932e-09	4.17743e-09	3.83302e-09	2.81434e-09	2.39829e-09

First, we consider the discrete problem (4.3). The range values for the parameter p^{-1} are between $\dfrac{E}{2(1+\nu)}$ and $\dfrac{500\ E}{2(1+\nu)}$. As a first guess we choose the penalized parameter $p^{-1} = \dfrac{\varepsilon E}{2(1+\nu)}$ that is of the same order as the coefficient of the shear energy for the analogous Naghdi's model, but we have observed in practice that this is not always the optimal choice, while very large values of p^{-1} may lead to wrong results. Hence for our tests, we take different values between a value close to the guess one up to a larger but relatively moderated one.

Table 1 shows the error at the origin for u_3^h and the maximum value for the constraint $\|r_h + (\partial_\alpha u_h \cdot a_3)a^\alpha\|^2$ using the formulation (4.3) with b. Table 2 shows the results using the scheme (5.4).

In Table 2 we observe that as p goes to 0 the error decreases and converges to the value 0.0001 for the scheme (5.4); whereas, according to Table 1 the total error deteriorates for the penalized problem (4.3) (see Figs. 5). This is due to the fact that the error is the sum of the error which comes from the penalty term, and

TABLE 2. Error and constraint using (5.4).

p^{-1}	1e04	5e04	1e05	5e05	1e06	1.5e06	5e06
Err	5.21561e-05	7.2932e-05	7.97911e-05	9.7089e-05	0.000104576	0.00010857	0.00011116
Maximum value for the constraint	3.7733e-09	3.7132e-09	3.9537e-09	4.7377e-09	5.0871e-09	5.2603e-09	5.3638e-09

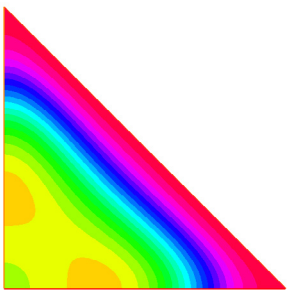

(A) isovalues for u_3, $p^{-1} = \dfrac{200E}{2(\nu+1)}$

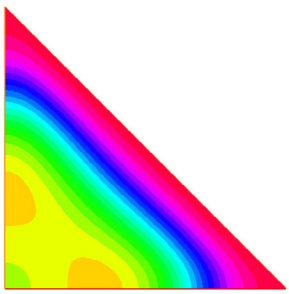

(B) isovalues for u_3, $p^{-1} = \dfrac{500E}{2(\nu+1)}$

FIGURE 4. Isovalues for u_3 using (5.4).

the error of interpolation (see (5.24)). In other words, we believe that both methods will give better results if a refined mesh is used. In Table 2 one can observe that some results are much better than the asymptotic ones, this is due to the fact that the error is evaluated on a single scalar quantity $u_3(0,0)$ and therefore errors may more easily cancel out and actually yield a better result.

As it is shown in Figures 2 and 3 the form of the isovalues changes when p decreases. Figures 4A and 4B show that the scheme (5.4) is stable when p goes to zero. For the constraint we observe that the penalty formulation (4.3) gives better results than (5.4) even if both methods give reasonable results for p sufficiently small.

Finally, in Figure 5, we display the error at the origin as a function of the parameter $1/p$. We observe that for the same mesh size and the same parameter $1/p$ the mixed method (5.4) gives better results than the scheme (4.3) when $1/p$ becomes very large.

6.2. Pinched cylinder

In this subsection we consider a model problem where the shell is a cylinder with freely supported ends. The problem data and geometry are illustrated in Figure 6. The midsurface is described by:

$$\varphi(x,y) = (x, R\cos(y), R\sin(y)), \quad -L \le x \le L, \quad 0 \le y \le \frac{\pi}{2}. \tag{6.3}$$

The shell is subjected to two centrally located and diametrically opposite forces of magnitude P at the center. Using the double symmetry of the structure and the load, only one eighth of the cylinder is analyzed.

Our numerical test is performed with a mesh containing 392 triangles, for $p^{-1} = 5.72769e+12$ and using the formulation (4.3) with P2-Lagrange elements. The plotted distributions of $Eu \cdot a_3$ presented in Figures 7, 8A and B are in good agreement with the results reported in [4, 9, 21]. In particular, in Table 3 we report some results at the points C, B and D. The values of the theoretical solution are given in [21] and once again our

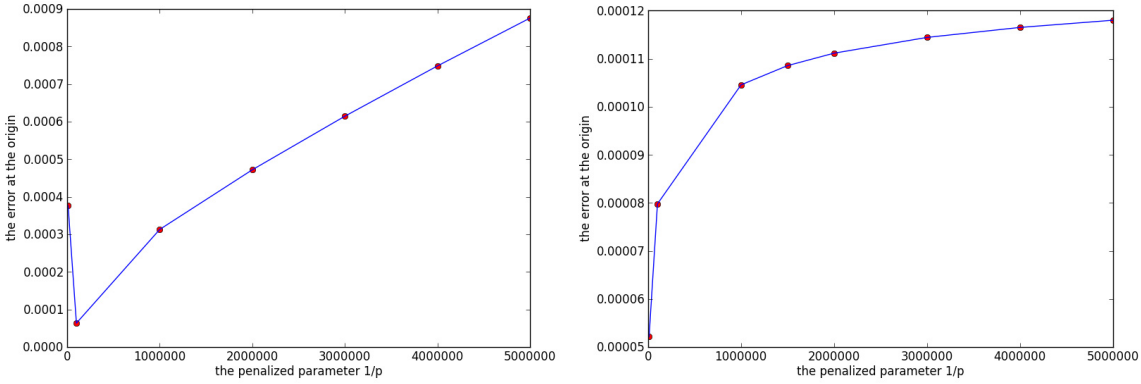

(A) The error at the origin as a function of $1/p$ using (4.3)

(B) The error at the origin as a function of $1/p$ using (5.4)

FIGURE 5.

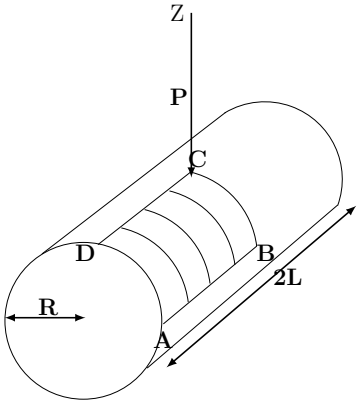

$E = 3 \times 10^7$ psi
$\nu = 0.3$
$\varepsilon = 1.0$ in
$R = 100$ in
$L = 100$ in
$P = 1$ lb

FIGURE 6. Cylindrical shell.

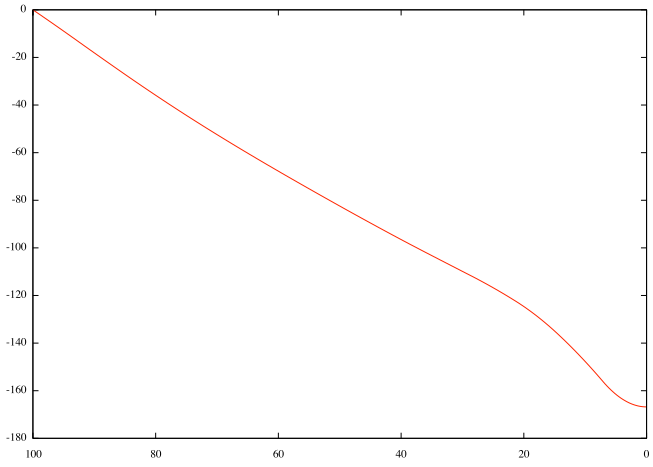

FIGURE 7. $E\ u \cdot a_3$ on DC.

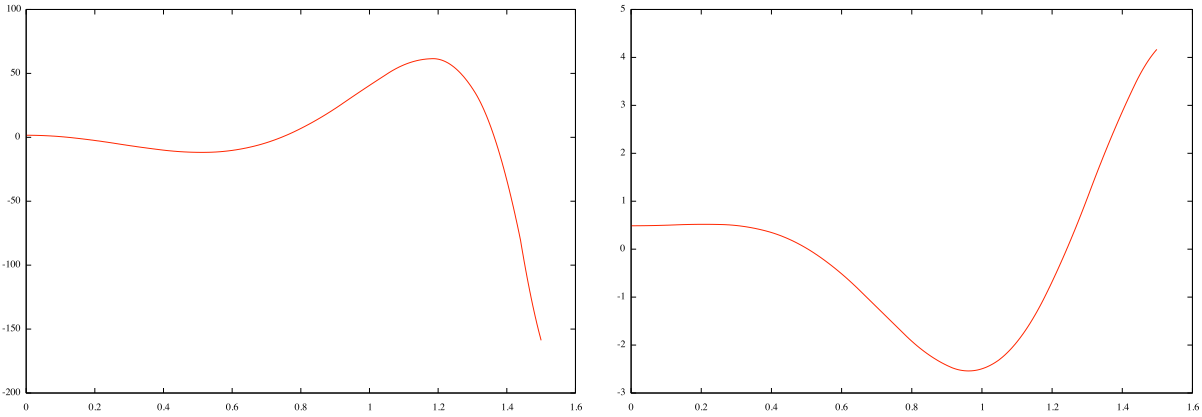

(A) $E\ u \cdot a_3$ on BC (B) $E\ u \cdot a_1$ on AD

FIGURE 8.

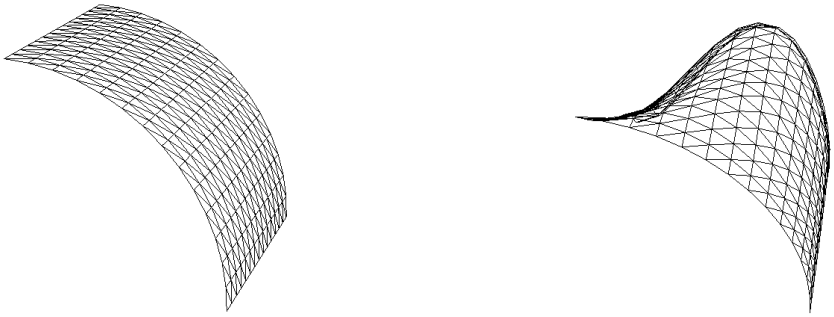

(A) An eight of the shell before deformation (B) An eight of the shell after deformation

FIGURE 9. An eight of the shell before and after deformation.

TABLE 3. Values of $E\ (u \cdot a_3)(C), E\ (u \cdot a_3)(B)$ and $E\ (u \cdot a_1)(D)$.

	[21]	(4.3)
$E\ (u \cdot a_3)(C)$	-164.24	-166.8
$E\ (u \cdot a_1)(D)$	4.14	4.35004
$E\ (u \cdot a_3)(B)$	-0.47	-0.478694

results are in good agreement with them. Finally Figure 9B represent the deformed configuration of an eight of the pinched cylinder for $0.5E\ u \cdot a_3$.

6.3. Bending dominant shell problems

The *membrane locking* phenomena may occur in shells, when the shell deforms by inextensional displacements. Since the tensor of change of metrics $\gamma_{\alpha\beta}$ vanishes for this type of displacements, the membrane energy vanishes, giving an exceedingly stiff behavior of the thin shell. Notice that in this case an appropriate scaled

solution converges to a well-defined limit, which is indeed a non-trivial inextensional displacement. Furthermore, the whole elastic energy is asymptotically stored in the bending part and the problem is said bending dominant. For such problem, standard finite element methods fail to give reasonable approximation for small values of the thickness ε. Several approaches have been developed to circumvent the locking phenomena, we refer to [1, 10, 13, 18, 22, 25].

For bending dominated shell problems, the proper load-scaling factor is 3.0, i. e., the load f is given by $f = \varepsilon^3 f_0$, where f_0 is independent of ε (see [2, 22]). Therefore, problem (2.24) is equivalent to the following one (changing the Dirichlet boundary conditions by $u = s = 0$ on a part γ_0 of $\partial\omega$):

Find $U \in \mathbb{X}(\omega) = \{(v,s) \in H^1\left(\omega, \mathbb{R}^3\right)^2, \partial_\alpha v \cdot a_3 \in H^1(\omega), v|_{\gamma_0} = s|_{\gamma_0} = 0\}$ such that:

$$\int_\omega \left(\frac{a^{\rho\sigma\alpha\beta}}{12} \chi_{\alpha\beta}(U)\, \chi_{\rho\sigma}(V) + \varepsilon^{-2} (a^{\rho\sigma\alpha\beta} \gamma_{\alpha\beta}(u)\, \gamma_{\rho\sigma}(v)) \right) \sqrt{a} \mathrm{d}x = \int_\omega f_0 v \sqrt{a}\, \mathrm{d}x. \tag{6.4}$$

We define the scaled energy as:

$$\begin{aligned} E_{sc} :=& \frac{1}{2} \int_\omega \left(\frac{a^{\rho\sigma\alpha\beta}}{12} \chi_{\alpha\beta}(U)\, \chi_{\rho\sigma}(U) + \varepsilon^{-2} (a^{\rho\sigma\alpha\beta} \gamma_{\alpha\beta}(u)\, \gamma_{\rho\sigma}(u)) \right) \sqrt{a} \mathrm{d}x \\ :=& \frac{1}{2} (a_b(U,U) + \varepsilon^{-2} a_m(u,u)). \end{aligned}$$

As it was mentioned in the beginning of this paper, the bilinear form from the left hand-side of (6.4) is not coercive on $\mathbb{X}(\omega)$. Hence following [1, 10, 25], we introduce "the membrane stresses" as independent unknowns,

$$\psi_{\alpha\beta} = (\varepsilon^{-2} - c_0) a^{\alpha\beta\rho\sigma} \gamma_{\rho\sigma}(U),$$

and propose to replace (6.4) by a penalized one using the bilinear form (3.4) or (3.5). In other words, we consider the following mixed problem:

$$\begin{cases} \text{Find } U = ((u,r), \underset{\approx}{\psi}) \in \mathbb{X}(\omega) \times \underset{\approx}{\boldsymbol{\Lambda}} \text{ such that} \\ \quad \mathcal{A}(U,V) + \mathcal{B}(\underset{\approx}{\psi}, V) = \mathcal{L}(V), \forall V = (v,s) \in \mathbb{X}(\omega), \\ \mathcal{B}(U,\phi) - \epsilon^2 \mathcal{C}(\underset{\approx}{\psi}, \underset{\approx}{\phi}) = 0, \forall \underset{\approx}{\phi} \in \underset{\approx}{\boldsymbol{\Lambda}}, \end{cases} \tag{6.5}$$

where we set

$$\begin{aligned} \underset{\approx}{\boldsymbol{\Lambda}} =& \{\underset{\approx}{\phi} = (\phi_{\alpha\beta})_{1\le\alpha,\beta\le 2}, \quad \phi_{\alpha\beta} \in L^2(\omega)\} \\ \mathcal{A}(U,V) =& \int_\omega \frac{a^{\rho\sigma\alpha\beta}}{12} \chi_{\alpha\beta}(U)\, \chi_{\rho\sigma}(V) \sqrt{a} \mathrm{d}x + c_0 \int_\omega a^{\rho\sigma\alpha\beta} \gamma_{\alpha\beta}(u)\, \gamma_{\rho\sigma}(v) \sqrt{a} \mathrm{d}x \\ & + p^{-1} \int_\omega (r + (\partial_\alpha u \cdot a_3) a^\alpha) \cdot (s + (\partial_\alpha v \cdot a_3) a^\alpha) \mathrm{d}x, \\ \mathcal{B}(\underset{\approx}{\psi}, V) =& \int_\omega a^{\alpha\beta\rho\sigma} \gamma_{\rho\sigma}(V) \psi_{\rho\sigma} \sqrt{a}\, \mathrm{d}x, \quad \text{when } \underset{\approx}{\psi} = \begin{pmatrix} \psi_{11} & \psi_{12} \\ \psi_{21} & \psi_{22} \end{pmatrix}, \\ \mathcal{C}(\underset{\approx}{\psi}, \underset{\approx}{\phi}) =& \int_\omega \psi_{\alpha\beta} \phi_{\alpha\beta}\, \mathrm{d}x \quad \text{and} \quad \epsilon = \frac{\varepsilon^2}{1 - c_0 \varepsilon^2}, \end{aligned}$$

and c_0 is an arbitrary positive constant independent of ε.

Its discrete couterpart is:

$$\begin{cases} \text{Find } U_h = ((u_h, r_h), \underset{\approx}{\boldsymbol{\psi}_h}) \in \mathbb{X}_h \times \underset{\approx}{\boldsymbol{\Lambda}_h} \text{ such that} \\ \quad \mathcal{A}(U_h, V_h) + \mathcal{B}(\underset{\approx}{\boldsymbol{\psi}_h}, V_h) = \mathcal{L}(V_h), \forall V_h = (v_h, s_h) \in \mathbb{X}_h, \\ \mathcal{B}(U_h, \phi_h) - \epsilon^2 \mathcal{C}(\underset{\approx}{\boldsymbol{\psi}_h}, \underset{\approx}{\boldsymbol{\phi}_h}) = 0, \forall \underset{\approx}{\boldsymbol{\phi}_h} \in \underset{\approx}{\boldsymbol{\Lambda}_h}. \end{cases} \tag{6.6}$$

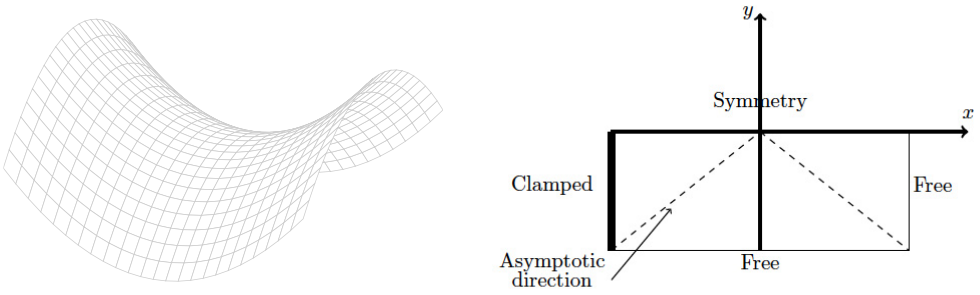

(A) The surface $S = \varphi(\omega)$ (B) Half of the domain

FIGURE 10.

TABLE 4. Energy values for P2 elements, $c_0 = 1$ and $p^{-1} = \frac{E\times 10^{-6}}{1+\nu}$.

$k = 2$	$\varepsilon = 0.1$	$\varepsilon = 0.01$	$\varepsilon = 0.001$	$\varepsilon = 0.0001$	$\varepsilon = 0.00001$
E_m	1.37911e-16	4.4088e-14	4.30382e-11	1.1677e-09	3.19627e-09
E_b	0.000374695	0.00037464	0.000374797	0.000374775	0.000374697
E_{sc}	0.000374695	0.00037464	0.000374797	0.000374776	0.0003747

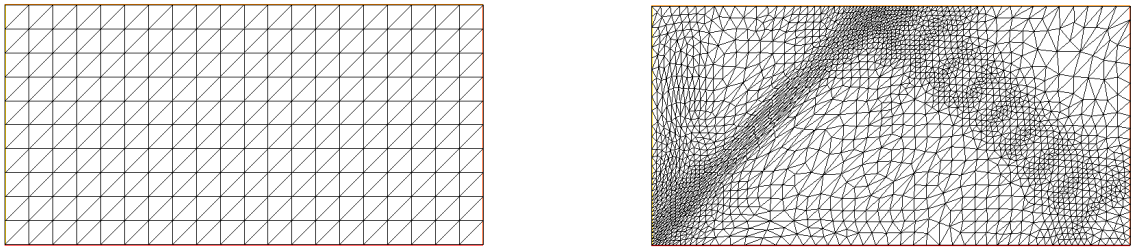

(A) Initial mesh (B) Adapted mesh

FIGURE 11. Initial and adapted meshes for $\varepsilon = 0.0001$

6.3.1. Partly clamped hyperbolic paraboloid shell problem

In order to assess the behaviour of our proposed method with respect to the locking, we consider the hyperbolic paraboloid test problem: Its midsurface is described by the equation

$$(x, y, x^2 - y^2), \quad (x, y) \in \omega = \left]-\frac{1}{2}, \frac{1}{2}\right[^2,$$

and is supposed to be clamped along the side $\gamma_0 = \{x = -1/2\}$. The scaled loading (force per unit area) is $80\varepsilon^3$, where ε is thickness of the shell. We here take Young's modulus $E = 2 \times 10^{11}$ and Poisson's ration $\nu = 0.3$. Note that, this example was already studied by [22] using MITC shell elements using the Naghdi shell model. For different values of p^{-1}, we compare our results with those obtained in [22]. Note that the asymptotic directions[6] of the surface S are $y = \pm x$.

In Table 4 we present the results of the scheme (6.6) for different values of thicknesses, using P2-Lagrange elements for all unknowns and a mesh made of 400 triangles. As we see, the numerical locking is avoided.

[6]The directions $(\mathrm{d}x, \mathrm{d}y)$ that cancel $b_{11}\mathrm{d}x^2 - 2b_{12}\mathrm{d}x\mathrm{d}y + b_{22}\mathrm{d}y^2$.

TABLE 5. Condition number for the penalized formulation with (3.5) and $\varepsilon = 0.1$.

h \ p	1.0e-4	1.0e-5	1.0e-6	1.0e-7
0.2	1.03e6	7.53e6	5.96e7	3.32e8
0.1	2.07e7	1.89e8	1.76e9	1.46e10
0.05	3.53e8	3.45e9	3.40e10	4.03e10

TABLE 6. The condition number for the penalized formulation with (3.5) and $h = 0.1$.

ε \ p	1.0e-4	1.0e-5	1.0e-6	1.0e-7
0.1	2.76e+07	2.50e+08	2.39e+09	2.04e+10
0.01	7.85e+08	8.20e+09	4.75e+10	1.55e+11
0.001	8.49e+09	4.83e+10	1.55e+11	3.28e+11

TABLE 7. The condition number for the penalized formulation with (3.5) and $p = 10^{-5}$.

ε \ h	0.2	0.1	0.05
0.1	1.1248e+08	5.4689e+08	2.6719e+09
0.01	4.8261e+08	2.1991e+09	9.5589e+09
0.001	1.0775e+09	1.3217e+10	6.6983e+10

The membrane energy is negligible compared to the bending energy for different values of the thickness, this means that the bending nature of the problem is well captured by the mixed discrete formulation (6.6). The membrane energy vanishes for decreasing thicknesses, whereas the bending energy becomes dominant: it can be scaled by a factor of ε^3 and the scaled energy converges to a constant value. The obtained results show that the bending energy is dominant, which corresponds to the asymptotic behavior of bending-dominated shells (see [2]). Figure 11B is obtained by P2-Lagrange element for $u_1, u_2, r_1, r_2, r_3, \psi_{11}, \psi_{12}, \psi_{22}$ and P3-Lagrange element for u_3. It shows how internal concentrated energy layers can develop in a shell structure, since we clearly observe that the energy concentrate along the asymptotic directions (characteristics) $y = \pm x$. After a sufficient number of refinements, boundary layer phenomena in the vicinity of the clamped part appears.

Finally Tables 5, 6 and 7 show the condition number of the corresponding matrix of the partly clamped hyperbolic paraboloid problem where the data are given in Section 6.3.1 using the penalized formulation (4.3) with (3.5) for different values of the parameter p, the thickness ε and the mesh size h. Based on these results, we can conjecture that the condition number of the matrix grows as $\approx \varepsilon^{-1} \times p^{-1} \times h^{-2}$, revealing a multiplicative effect between the thickness of the shell and the penalization parameter. But since we are considering two-dimensional problems, this effect does not affect our numerical results.

7. CONCLUDING REMARKS

In this work, the first considered approach is a penalized formulation of the Koiter model for a linear elastic shell and its approximation by a "non conforming" finite element method. It is based on the same principle (in a weak sense) such as the DKT finite element but with a large possible choice of polynomial spaces. We have derived an abstract *a priori* error estimates in the energy norm. The convergence results and some concrete error estimates of the method are stated. The advantage for considering closed penalty stays on the continuous problem because it leads to error of order $O(p)$ (as the penalized parameter $p \to 0$) instead of an error of order $\sqrt{p}$. The second approach that we have considered is a mixed formulation based on this closed penalized formulation for which we are able to prove that it converges uniformly with respect to the penalized parameter

and the mesh size; hence this method is robust with respect to p. Indeed, if the bilinear form (3.5) is used (which leads to non closed penalization), the error deteriorates as p goes to zero. Another advantage of the proposed method is the fact that we can use very simple elements (in our numerical experiments we have used P2 Lagrange elements for both displacement and rotation unknowns). This approach has been illustrated with good numerical results.

For Koiter's model, membrane locking can occur when the thickness goes to zero, its approximation by robust and accurate mixed finite element methods was considered in [1,10,25]. We have proposed a "'penalized-mixed" method and have tested it for the partly clamped hyperbolic paraboloid shell problem. This is a bending dominated benchmark problem that allows to test whether a finite element procedure locks or not ([22]). At least for the chosen benchmark (Sect. 6.3), we have seen that combining the two techniques lead to a robust method in the sense that it does not suffer from the "membrane locking". A rigorous analysis of this new method is postponed to future works.

References

[1] D.N. Arnold and F. Brezzi, Locking-free finite element method for shells. *Math. Comput.* **66** (1997) 1–14.

[2] F. Auricchio, L. Beirão da Veiga and C. Lovadina, Remarks on the asymptotic behaviour of koiter shells. *Comput. Struct.* **80** (2002).

[3] I. Babuska, The finite element method with penalty. *Math. Comput.* **27** (1973) 221–228.

[4] M. Bernadou, Méthode d'élements finis pour les problèmes de coques minces. Dunod (1994).

[5] C. Bernardi, A. Blouza, F. Hecht and H. Le Dret, A posteriori analysis of finite element discretizations of a Naghdi shell model. *IMA. J. Numer. Anal.* **33** (2013) 190–211.

[6] A. Blouza, L. El Alaoui and S. Mani−Aouadi, *A posteriori* analysis of penalized and mixed formulations of Koiter's shell model. *J. Comput. Appl. Math.* **296** (2016) 138–155.

[7] A. Blouza and H. Le Dret, Existence and uniqueness for the linear Koiter shell model with little regularity. *Quarterly Appl. Math.* **57** (1999) 317–338.

[8] A. Blouza, F. Hecht and H. Le Dret, Two finite element approximations of Naghdi's shell model in Cartesian coordinates. *SIAM J. Numer. Anal.* **44** (2006) 636–654.

[9] K.-J. Bathe and L.-W. Ho, A simple and effective element for analysis of general shell structures. *Comput. Struct.* **13** (1981).

[10] J.H. Bramble and T. Sun, A locking-free finite element method for Naghdi shells. *J. Comput. Appl. Math.* **89** (1997) 119–133.

[11] S.C. Brenner and L.R. Scott, The Mathematical Theory of Finite Element Methods. Springer Verlag, New York (2008).

[12] H. Brezis, Analyse fonctionnelle, Théorie et applications. *Mathématiques Appliquées pour la Maîtrise*. Masson, Paris (1983).

[13] D. Chapelle and R. Stenberg, Stabilized finite element formulations for shells in a bending dominated state. *SIAM J. Numer. Anal.* **36** (1998) 32–73.

[14] Ph.G. Ciarlet, The Finite Element Method for Elliptic Problems. *Studies in Mathematics and its Applications*. North-Holland Amsterdam (1978).

[15] Ph.G. Ciarlet, Mathematical elasticity. Theory of shells. III. Vol. 29 of *Studies in Mathematics and its Applications*. North-Holland Publishing Co., Amsterdam (2000).

[16] M. Dauge and E. Faou, Koiter estimate revisited. *Math. Models Methods Appl. Sci.* **20** (2010) 1–42.

[17] F. Hecht, New development in freefem++. *J. Numer. Math.* **20** (2010) 251–265.

[18] J. Pitkäranta, Y. Leino, O. Ovaskainen and J. Piila, Shell deformation states and the finite element method: a benchmark study of cylindrical shells. *Comput. Methods Appl. Mech. Eng.* **181** (1995) 81–121.

[19] W.T. Koiter, On the foundations of the linear theory of thin elastic shells. Number B73 in Wetensch. *Proc. Kon. Ned. Akad* (1970).

[20] J.L. Lions. Quelques méthodes de résolution des problèmes aux limites non linéaires. Dunod-Gauthier-Viltars Paris (1969).

[21] G.M. Lindberg, M.D. Olson and G.R. Cowper, New developments in the finite element analysis bf shells. *Ouart. Bull. Div. Mech. Comput.* **4** (1969).

[22] P.-S. Lee and K-J. Bathe, On the asymptotic behavior of shell structures and the evaluation in finite element solutions. *Comput. Struct.* **80** (2002).

[23] B. Maury, Numerical analysis of finite element/volume penalty method. *SIAM J. Numer. Anal.* **47** (2009) 1126–1148.

[24] P.M. Naghdi, Foundations of elastic shell theory. In Vol. IV of *Progress in Solid Mechanics*. North-Holland, Amsterdam (1963) 1–90.

[25] T. Sun, A locking-free mixed finite element method for the Koiter shell model. In *Proc. of The 3rd IMACS Inter. Symp. Iterative Methods Sci. Comput.* Edited by Jackson Hole. Wyoming (1977) 307–312.